

STUDY ON CLOUD CLASSIFICATIONS BY USING AVHRR, GMS-5 AND TERRA/MODIS SATELLITE DATA*

SHI Chunxiang (师春香)**, ZHANG Wenjian (张文建),

ZHANG Liyang (张里阳) and GUO Wei (郭伟)

National Satellite Meteorological Center, Beijing 100081

Received March 15, 2002; revised May 21, 2002

ABSTRACT

This paper presents the automated pixel-scale neural network classification methods being developed at National Satellite Meteorological Center (NSMC) of China to classify clouds by using NOAA/AVHRR and GMS-5 satellite imageries. By using Terra satellite MODIS imageries, an automated pixel-scale threshold technique has been developed to detect and classify clouds. The study focuses on applications of these cloud classification techniques to the Huaihe River and the Changjiang (Yangtze) River drainage basin. The different types of clouds show more clearly on this cloud classification image than single band image. The results of the cloud classifications are the basis of studying cloud amount, cloud top height and cloud top pressure. Cloud mask methods are widely used in SST, LST, and TPW retrieval schemes. Some case studies about cloud mask and cloud classification in satellite imageries, which are related with the study of Global Energy and Water Cycle Experiment (GEWEX) in the Huaihe River and the Changjiang River drainage basin are illustrated.

Key words: cloud mask and classification, neural network, satellite imagery, MODIS data

I. INTRODUCTION

Cloud mask algorithms are based on the fact that the spectral behavior of clouds and earth's surfaces are different in window channels. Higher reflectance and lower temperature than the underlying surface generally characterize clouds. The main difficulties of cloud detecting are that the earth's surface characteristics (which vary with the surface type, the atmospheric conditions, the sun and satellite respective positions) are very complex so that the contrast between the cloud and earth's surface characteristics may be very low under certain circumstances. In addition, some cloud types such as thin cirrus, low stratus at night, and small cumulus are difficult to detect because of insufficient contrast with the surface radiance. Cloud edges cause the further difficulty since the instrument field of view will not always be completely cloudy or clear.

Three techniques may be applied to cloud detection. Clustering techniques, which are scene dependent methods, mainly use pixel values of the entire scene through histogram

* Supported by the National Natural Science Foundation of China (49794030).

** E-mail: shicx@nsmc.cma.gov.cn

analysis or other calculations to segment the image according to pre-defined rules; Artificial neural networks, the advanced multidimensional regression techniques, are capable of treating predictions and predictors in a very flexible way (allowing nonlinear relations): Multi-spectral threshold techniques are based on pixel-by-pixel analysis of radiance where cloud-free and cloudy pixels are identified if pixel radiance can pass a sequence of threshold tests. The chosen method should be efficient in term of computing time, make the maximum use of channels, be easily adapted (e. g., if one channel is missing), and be mature. Moreover, it should be possible to easily tune the algorithm. The clustering techniques have been considered to be too scene-dependent. Artificial neural network techniques are promising methods, but it is sensitive to the learning data set (see Atkinson and Tatnall 1997; Foody and Arora 1997; Peak and Tag 1994). One of the main advantages of the multi-spectral threshold technique is that it is relatively easy to adapt thresholds to varying meteorological conditions, earth's surface types, viewing geometry using external data, for example, Numerical Weather Prediction (NWP) model forecasting, Radiation Transfer Model (RTM) calculations, climatological atlas (see Michel et al. 1982; Hutchison and Hardy 1995; Ackerman et al. 1990). This physical approach will also allow an easy tuning of the cloud mask prototypes to other spectral characteristics. One of the main disadvantages is that the thresholds need to be tuned frequently.

This paper first presents the automated pixel-scale neural network methods being developed in NSMC to do cloud detection and cloud classification. The data set used in this study is mainly from Advanced Very High Resolution Radiometer (AVHRR), the Geostationary Meteorological Satellite (GMS) imageries. Then the automated pixel-scale threshold cloud detection and classification technique is presented by using Earth Observing Satellite (EOS) Moderate Resolution Imaging Spectroradiometer (MODIS) imageries.

II. NOAA/AVHRR NEURAL NETWORK CLOUD CLASSIFICATION TECHNIQUES

The field of neural networks can be thought of as being related to artificial intelligence, machine learning, parallel processing, statistics, and other fields. The attraction of neural networks is that they are best suited to solving the problems that are the most difficult to solve by traditional computational methods. We use the Back-Propagation (BP) neural network in this cloud classification study, which is widely used in many fields.

The BP learning process works in small iterative steps: one of the example cases is applied to the network, and the network produces some output based on the current state of its synoptic weights (initially, the output will be random). This output is compared to the known-good output, and a mean-squared error signal is calculated. The error value is then propagated backwards through the network, and small changes are made to the weights in each layer. The weight changes are calculated to reduce the error signal for the case in question. The whole process is repeated for each of the example cases, then back

to the first case again, and so on. The cycle is repeated until the overall error value drops below some pre-determined thresholds. At this point we say that the network has learned the problem "well enough" —the network will never exactly learn the ideal function, but rather it will asymptotically approach the ideal function.

AVHRR has five channel's of visible, near-infrared, and thermal infrared spectrum. The channel's spectrum characteristics are: channel 1, 0.58–0.68 μm , channel 2, 0.725–1.10 μm , channel 3, 3.55–3.93 μm , channel 4, 10.3–11.3 μm and channel 5, 11.5–12.5 μm , respectively. The AVHRR Global Area Coverage (GAC) data provide collection of data from all spectral channels for globe, and worldwide users can receive HRPT direct broadcasting data stream locally. Each pass of the satellite provides a 2399 km (1491 m) wide swath. The satellite orbits the earth and measures the temperature of clouds and the surface. The AVHRR applications have extended far beyond the original objectives, however, simple mapping of cloud patterns is still an important application, especially at high latitudes where data from geostationary satellites are severely distorted (due to earth curvature).

In this study, the sample database of clouds, land and water is built based on AVHRR 5 channel's data which include more than thirty thousand 8×8 pixel samples and more than twenty thousand one pixel samples. Theory analysis and experiment show that not only 5 channel's data can be used to distinguish clouds and land and water but also the band combination with each other can do so. For example, the differences of AVHRR channels 4 and 5 can be used to distinguish water particle cloud and ice particle cloud because the biggest absorption difference between water particles and ice particles is near 12 μm . Based on theory analyses and experiments, 80 features are extracted from 5 channel's AVHRR data for 8×8 pixel samples, which involve spectrum features, gray features, channel difference features and the gray scale statistical features. 20 features are selected using step-by-step distinguishing analysis method, which includes spectrum features, gray features. 20 features are extracted from 5 channel AVHRR data for single pixel samples.

The inputs of our AVHRR automatic cloud classification system are 5 AVHRR channel's data and outputs are classified gray images. Cloud classified images involve cumulonimbus, cumulus congestus, cumulus, cirrus, middle cloud, low cloud and land, water and unknown pixel.

Cloud classification experiment by sample database is done using neural network method. This neural network model has 20 input nodes, 2 hidden layers and 4 output nodes (20-40-15-4). More than three thousand samples selected randomly are used to train the neural network model. The other independent samples are used for testing. Testing result shows that classification accuracy is about 78% for single pixel sample database and 79% for 8×8 pixel sample database. Table 1 shows classification experiment results. Generally classification accuracy of 8×8 pixel samples is a little better than single pixel samples, but when neural network model is used in the practical application to one satellite image, the single pixel cloud classification neural network model is better.

Table 1. Single Pixel Cloud Classification Experiment Results

Calcula- tion fact	1	2	3	4	5	6	7	8	9	Right sample number s	Total numbers of each type	Accu- rate ratio %
1	2207	157	25	335	21	0	0	0	45	2207	2835	77.0
2	158	1119	41	457	0	0	0	0	158	1119	2091	53.0
3	29	3	684	76	133	223	121	0	0	684	1269	53.0
4	145	214	3	7186	435	0	3	0	194	7186	8374	85.0
5	38	6	10	450	1822	1	47	0	13	1822	2400	75.0
6	8	0	554	107	126	1648	413	0	0	1648	2856	57.0
7	1	0	5	0	2	0	1935	33	6	1935	1982	97.0
8	0	1	2	0	1	1	28	330	13	330	376	87.0
Total accurate ratio of cloud classification						77.8%						

Figure 1 (consisting of diagrams (a, b), see plate at page 402) is a cloud classification case study using trained neural network model. Fig. 1a is the classified color image of NOAA-11 at 0500 UTC 20 July 1992, the range is 30–35°N, 140–145°E, located in the northeast region of HUBEX experiment area. Figure 1b is channel-4 cloud image at the same time. In this case, cumulonimbus (red), cumulus congestus (purple), cumulus humilis (light purple), cirrus (cyan), middle cloud (yellow), low cloud (pink), land (green), water (blue), and unknown (white) are all marked. But some of multiple level clouds and boundary pixels are not recognized because of having no such samples in learning sample set.

III. GMS-5 NEURAL NETWORK CLOUD CLASSIFICATION TECHNIQUES

The GMS series are satellites in geostationary orbit at 140°E. Monitoring weather conditions, they are one link in World Weather Watch sponsored by the World Meteorological Organization. Observation data consisting of cloud distribution pictures sent from these satellites are used in many fields including TV and newspaper weather forecasts. GMS-5 has four channels of visible and thermal infrared spectrum. The channels spectrum characteristics are: channel 1, 0.55–0.90 μm , channel 2, 6.5–7.0 μm , channel 3, 10.5–11.5 μm , and channel 4, 11.5–12.5 μm .

Sample database of clouds, land and water is built based on GMS-5 four-channel data which include several thousands of one pixel samples. Sample database is collected from the GMS-5 satellite imageries from June to August 1998. GMS-5 has two window channels with little atmospheric absorption. They can show thermal characters of surface well. The water vapor channel detects middle-high level water vapor in the atmosphere.

Additionally there is a visible band. Theory analysis and experiment show that not only four-channel data can be used to distinguish clouds, lands and water but also the difference between channels can do so. For example, the brightness temperature difference between channel 3 and channel 4 can be used to distinguish thin cirrus. On the basis of theory analyses and experiment, 20 features are selected as the input of the cloud classification neural network model.

Figure 2 (consisting of diagrams (a, b, c), see plate at page 402) is a cloud classification case study using trained neural network model. Fig. 2a is the infrared channel (channel 3) satellite imagery of GMS-5 at 0600 UTC 24 June 1999, the region is 0–60°N, 70–150°E. Figure 2b is the visible (channel 1) satellite imagery at the same time. Figure 2c is the GMS-5 cloud classified color image at the same time. In this case, water, land, low-level cloud, middle-level cloud, multi-level cloud, cirrus and cumulonimbus are shown with different color. The low-level cloud in the up-right of the imagery is clearly shown in the classification image but it is hard to be distinguished in the infrared imagery. Over the Huaihe River and the Changjiang (Yangtze) River drainage basin there is a Meiyu front cloud system lasting from June 22 to July 3.

IV. MODIS CLOUD MASK AND CLOUD CLASSIFICATION USING MULTI-SPECTRAL THRESHOLDING TECHNIQUE

1. MODIS Data

The 36 channel MODIS data offer the opportunity for multi-spectral approaches to cloud mask and cloud classification more accurately. The spectrum characteristics of the 36 channels are shown in Table 2. MODIS cloud mask and classification algorithm are very complex.

2. Cloud MASK and Classification Methods for MODIS

The multi-spectrum threshold algorithm is applied to MODIS imagery for cloud mask and classification. For nomenclature, we shall denote the satellite measured solar reflectance as R , and refer to the infrared radiance as brightness temperature (equivalent blackbody temperature determined using the Planck function) denoted as BT . Subscripts refer to the wavelength at which the measurement is made. The multiple threshold cloud mask and cloud classification algorithm are to start with single pixel (1000 m field of view) tests. Thresholds are changed with space and time.

(1) Characteristic analysis on some of the MODIS bands

MODIS has a unique capability since it has measurements at three wavelengths in the window, 8.6, 11, and 12 μm . Three spectral regions mentioned are very useful in determination of cloud free atmospheres. Because the index of refraction varies quite markedly over this spectral region for water, ice, and minerals common to many naturally occurring aerosols, the effect on the brightness temperature of each of the spectral regions is different, depending on the absorbing constituent.

Table 2. MODIS Bands Used in the MODIS Cloud Mask Algorithm

Band	Wavelength (μm)	Yes/No	Used in cloud mask
1 (250 m)	0.659	Y	(250 m and 1 km) clouds, shadow
2 (250 m)	0.865	Y	(250 m and 1 km) low clouds
3 (500 m)	0.470	N	
4 (500 m)	0.555	Y	snow
5 (500 m)	1.240	Y	shadow
6 (500 m)	1.640	Y	snow
7 (500 m)	2.130	Y	aerosol
8	0.415	N	
9	0.443	N	
10	0.490	N	
11	0.531	N	
12	0.565	N	
13	0.653	N	
14	0.681	N	
15	0.750	N	
16	0.865	N	
17	0.905	N	
18	0.936	Y	low cloud
19	0.940	Y	shadow
20	3.750	Y	cloud
21/22	3.959	N (21) / Y (22)	window, shadow
23	4.050	Y	shadow
24	4.465	N	
25	4.515	N	
26	1.375	Y	thin cirrus
27	6.715	Y	high cloud
28	7.325	N	
29	8.550	Y	cloud
30	9.730	N	
31	11.030	Y	cloud
32	12.020	Y	cloud
33	13.335	N	
34	13.635	N	
35	13.935	Y	high cloud
36	14.235	N	

As a result of the relative spectral uniformity of surface emittance in the IR, spectral tests within various atmospheric windows (such as bands 29, 31, 32 at 8.6, 11, and 12 μm , respectively) can be used to detect the presence of cloud. Differences between BT_{11} and BT_{12} are widely used for cloud screening with AVHRR measurements, and this

technique is often referred to as the split window technique. Kriebel and saunders (1988) used $BT_{11} - BT_{12}$ differences to detect cirrus clouds — brightness temperature differences are greater over thin clouds than over clear or overcast conditions. Cloud thresholds are set as a function of satellite zenith angle and the BT_{11} brightness temperature (Spinhirne et al. 1996; Strabala et al. 1994).

In difference techniques, the measured radiances at two wavelengths are converted to brightness temperatures and subtracted. Because of the wavelength dependence of optical thickness and the non-linear nature of the Planck function (BT), the two brightness temperatures are often different. The basis of the split window and tri-spectral technique for cloud mask lies in the differential water vapor absorption that exists between different window channel (8.6 and 11 μm and 11 and 12 μm) bands. These spectral regions are considered to be part of the atmospheric window, where absorption is relatively weak. Most of the absorption lines are the result of water vapor molecules, with a minimum occurring around 11 μm . Since the absorption is weak, BT_{11} can be corrected for moisture absorption by adding the scaled brightness temperature difference of two spectrally close channels with different water vapor absorption coefficients: the scaling coefficient is a function of the differential water vapor absorption between the two channels. This is the basis for sea surface temperature (SST) retrieval.

A tri-spectral combination of observations at 8.6, 11 and 12 μm is suggested for detecting cloud properties by Ackerman et al. (1990). Strabala et al. (1994) further explored this technique by utilizing very high spatial-resolution data from MAS (MODIS Airborne Simulator). The physical premise of the technique is that ice and water vapor absorption peaks are in opposite halves of the window region: so that positive 8.6 minus 11 μm brightness temperature differences indicate cloud while negative differences, over oceans, indicate clear regions. The relationship between the two brightness temperature differences and clear-sky has also been examined using collocated HIRS (High Resolution Infrared Radiation Sounder) and AVHRR GAC global ocean data sets. As the atmospheric moisture increases, $BT_{8.6} - BT_{11}$ decreases while $BT_{11} - BT_{12}$ increases.

CO_2 slicing (Smith and Platt 1978; Wylie and Menzel 1989) is a useful method for sensing cloud amount and the height of clouds. Simple tests using the CO_2 channels are useful for cloud mask, particularly high clouds. Whether a cloud is sensed by these bands (MODIS bands 33–36) is a function of the weighting function of the particular channel and the altitude of the cloud. MODIS band 35 (13.9 μm) provides good sensitivity to the relatively cold regions of the atmosphere. Only clouds above 500 hPa will have strong contributions to the radiance to space observed at 13.9 μm ; negligible contributions come from the earth's surface. Thus a threshold test for cloud versus ambient atmosphere and a histogram test should reveal clouds above 500 hPa.

Visible reflectance test is a single channel test whose strength is discriminating to bright clouds over dark surfaces (e.g., stratus over ocean) and weakness is clouds over bright surfaces (e.g., snow). Two different channels are used in this test dependent on the ecosystem. The 0.66 μm (band 1) is used over oceans, land and snow/ice regions. The 0.88 μm reflectance test is also applied over snow/ice and desert scenes.

The reflectance ratio test uses channel 2 divided by channel 1 ($R_{0.87}/R_{0.66}$). This test

makes use of the fact that the spectral reflectance at these two wavelengths is similar over clouds (ratio is near 1) and different over water and vegetation. Using AVHRR data this ratio has been found to be between 0.9 and 1.1 in cloudy regions. If the ratio falls within this range, cloud is indicated.

Clouds that are low in the atmosphere are often difficult to detect with infrared techniques. The thermal contrast between clear-sky and low cloud is small and sometimes undetectable. Reflectance techniques, including the reflectance ratio test can be applied during daylight hours over certain ecosystems. Use of the MODIS band 18 at $0.936 \mu\text{m}$ also offers help under daytime viewing conditions. Gao and Goetz (1991) proposed a ratio test using spectral channels near 0.94 , 1.04 , and $1.14 \mu\text{m}$. Reflectance of many surfaces is linear between these wavelengths while absorption by water vapor is different across this spectral region, allowing discrimination between cloud and the ground using a band ratio $(R_{0.94} + R_{1.14})/2R_{1.04}$. MODIS does not have channels at these three wavelengths; however, other water vapor channels in the near-infrared may prove useful for cloud detection over land. A reflectance ratio of band 18 to band 16 ($0.865 \mu\text{m}$, an atmospheric window with surface reflectance characteristics similar to channel 18) could be used.

The physical principle detecting snow using $1.64 \mu\text{m}$ is the fact that the differences in reflected solar radiation between the 0.645 and $1.64 \mu\text{m}$ bands contain information regarding cloud particle phase due to distinct differences in bulk absorption characteristics between water and ice at the longer wavelength. The visible reflectance, suffering no appreciable absorption for either ice or liquid water, is relatively unaffected by thermodynamic phase. However, if the cloud is composed of ice, or if the surface is snow covered (similar in effect to large ice particles), then the reflectance of the cloud at $1.64 \mu\text{m}$ will be smaller than that for an otherwise identical liquid water cloud (Strabala et al. 1994; Smith and Platt 1978; Wylie and Menzel 1989).

The detection of cloud shadows is a problem. Clear-sky scenes that are potentially affected by shadows can be theoretically computed given the viewing geometry, solar azimuth and zenith angles, cloud edges distribution and cloud altitude. This approach requires too much CPU, and all the information (e.g., cloud altitude) is not available to the cloud mask algorithm. Therefore, as with clouds, solar reflectance tests can be explored for a cloud shadow detection algorithm. For MODIS data, the cloud masking algorithm checks for shadows can be based on reflectance at 0.94 , 0.87 and $0.66 \mu\text{m}$. A shadow is determined at present if $R_{0.936} < 0.12$ and $R_{0.87}/R_{0.66} > 0.9$ (Tsonis 1984; Yamanouchi et al. 1987).

Over land during the day, $BT_{3.9} > BT_{4.0}$ because there is more reflected solar energy at $3.9 \mu\text{m}$. In shadowed regions the incident solar radiation at $3.9 \mu\text{m}$ is reduced, and the brightness temperature differences are smaller. The issues of shadows caused by mountainous terrain also need studying. These shadows would be directly calculated from digital elevation maps, solar geometry considerations, and the cloud mask. The first two considerations would indicate the field of view where terrain shadow could occur; the last would determine whether sunlight is available to cause the shadow (Rossow et al. 1993).

(2) *Cloud mask and cloud classification test cases*

A simple cloud mask test is done using some thresholds as follows: BT_{11} , $BT_{11} - BT_{12}$, $BT_{11} - BT_{8.6}$, $BT_{13.9}$, $R_{0.66}$, $R_{0.87}$, $R_{0.87} / R_{0.66}$, and $R_{1.6}$. By applying one of these thresholds, a pixel will be classified as cloud or non-cloud. Different thresholds of testing give different results. When multi-threshold method is applied, pixel will be classified as cloud if most of the thresholds of testing flag this pixel as cloud. After above processing, land-sea mask data are applied to imagery to distinguish the land and water body. Figure 3 (see plate at page 403) is an example of the cloud mask using MODIS data over China (6 July 2001). The left image is the composed image of band 1, band 2 and band 4 and the right one is cloud mask image, green regions are land, blue regions are water, white areas are cloudy.

These thresholds, BT_{11} , $BT_{11} - BT_{12}$, $R_{0.66}$, $R_{1.6}$, and $BT_{13.9}$, are used in the cloud classification test on the basis of cloud mask. Figure 4 (see plate at page 403) is an example of the cloud classification using MODIS data over China (6 July 2001). The left image is the composed image of band 1, band 2 and band 31 and the right one is a cloud classified imagery. In the cloud classified imagery, the green regions are land, blue regions are water, white cumulonimbus, cyan areas are cirrus, and dark yellow areas are low-level cloud. Over the Changjiang River drainage basin there is the outer cloud system of the tropical cyclone.

V. CONCLUSIONS

This paper discussed cloud mask and cloud classification methods using the different satellite data. Some conclusions can be drawn from the study as follows:

(1) The different cloud classification methods have their advantage and disadvantage. In this paper we discussed the automated pixel-scale neural network method and the automated pixel-scale multi-spectrum threshold technique to detect and to classify clouds. For neural network cloud classification methods it has higher classification accuracy for one better sample database, but if some case did not occur in this sample database the neural network model can not recognize it. A perfect sample database including almost all cases in different seasons and different areas will need large resources. For pixel-scale multi-spectrum threshold technique it is relatively easy to adapt thresholds to varying meteorological conditions, earth's surface types, and viewing geometry using external data. One of the main disadvantages is that the thresholds need to be tuned frequently.

(2) Using MODIS data, we can distinguish between cloud-free and cloudy situations more exactly and recognize the different types of clouds more easily. Snow and low cloud is more easily distinguished using MODIS band 6 ($1.64 \mu\text{m}$), and band 6 is helpful for distinguishing between the ice cloud and water cloud. MODIS has measurements at three wavelengths in the window, 8.6, 11, and $12 \mu\text{m}$, which is very useful in determination of cloud-free atmospheres, and their combination is helpful in determining the thin cirrus.

(3) It shows that pixel-scale methods are more suitable for practical application than 8×8 pixel scale methods through testing using AVHRR data. Generally classification accuracy of 8×8 pixel samples is a little better than single pixel sample, but when neural

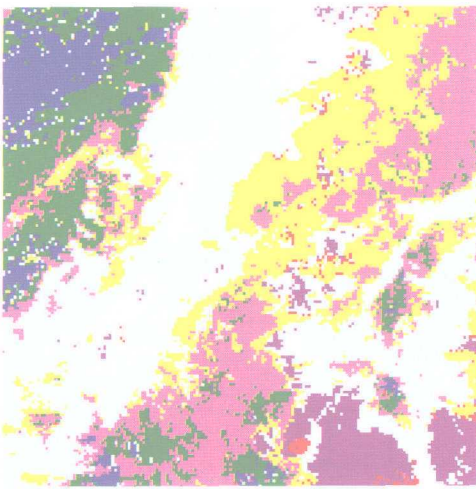
network model is used in the practical satellite image, the single pixel cloud classification neural network model is better.

(4) Although the spatial resolution of the GMS-5 data is lower than AVHRR and MODIS data, its higher time resolution makes it reflect weather system evolution process better. It can show clearly that the mesoscale convective cloud clusters in the Meiyu front evolve with time.

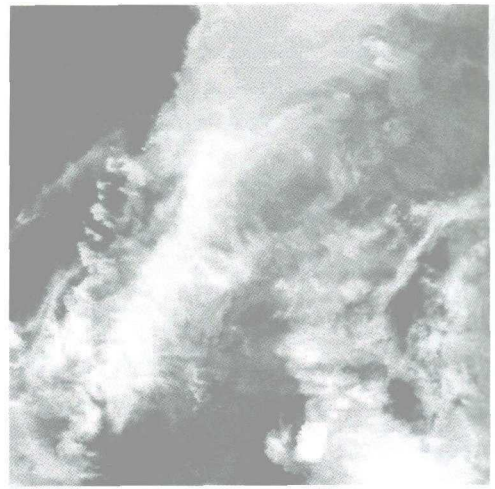
(5) Cloud mask result is the foundation of other studies such as SST and LST (land surface temperature), TPW (total precipitable water) retrieval and vegetation study using these satellite data. The output of cloud classification can be used to modify the NWP output cloud.

REFERENCES

- Ackerman, S. A., Smith, W. L. and Revercomb, H. E. (1990), The 27–28 October 1986 FIRE IFO cirrus case study: Spectral properties of cirrus clouds in the 8–12 micron window, *Mon. Wea. Rev.*, **118**: 2377–2388.
- Atkinson, P. M. and Tatnall, A. R. L. (1997), Introduction: Neural networks in remote sensing, *Inter. J. Remote Sensing*, **18**: 699–710.
- Foody G. M. and Arora, M. K. (1997), Remote sensing image analysis using a neural network and knowledge-based processing, *Inter. J. Remote Sensing*, **18**: 811–828.
- Gao, B. C. and Wiscombe, W. J. (1994), Surface-induced brightness temperature variations and their effects on detecting thin cirrus clouds using IR emission channels in the 8–12 micron region, *J. Appl. Meteor.*, **33**: 568–570.
- Gao, B. C. and Goetz, A. F. H. (1991), Cloud area determination from AVIRIS data using water vapor channels near $1\mu\text{m}$, *J. Geophys. Res.*, **96**: 2857–2864.
- Hutchison, K. D. and Hardy, K. R. (1995), Threshold functions for automated cloud analyses of global meteorological satellite imagery, *Inter. J. Remote Sensing*, **16**: 3665–3680.
- Kriebel, K. T. and Saunders, R. W. (1988), An improved method for detecting clear sky and cloudy radiances from AVHRR data, *Inter. J. Remote Sensing*, **9**: 123–150.
- Michel Desbois, Genevieve Seze and Gerard Szejwach (1982), Automatic classification of clouds on METEOSAT imagery: Application to high-level clouds, *J. Appl. Meteor.*, **21**: 401–412.
- Peak, J. E. and Tag, P. M. (1994), Segmentation of satellite imagery using hierarchical thresholding and neural networks, *J. Appl. Meteor.*, **33**: 605–616.
- Rossow, W. B., Walker, A. W. and Garder, L. C. (1993), Comparison of ISCCP and other cloud amounts, *J. Climate*, **6**: 2394–2418.
- Spinhirne, J. D., Hart, W. D. and Hlavka, D. L. (1996), Cirrus infrared parameters and shortwave reflectance relations from observations, *J. Atmos. Sci.*, **53**: 1438–1458.
- Smith, W. L. and Platt, C. M. R. (1978), Intercomparison of radiosonde, ground-based laser, and satellite deduced cloud heights, *J. Appl. Meteor.*, **17**: 1796–1802.
- Strabala, K. I., Ackerman, S. A. and Menzel, W. P. (1994), Cloud properties inferred from 8–12 μm data, *J. Appl. Meteor.*, **33**: 212–229.
- Tsonis, A. A. (1984), On the separability of various classes from GOES visible and infrared data, *J. Clim. Appl. Meteor.*, **23**: 1393–1410.
- Wylie, D. P. and Menzel, W. P. (1989), Two years of cloud cover statistics using VAS, *J. Climate*, **2**: 380–392.
- Yamanouchi, T., Suzuki, K. and Kawaguci, S. (1987), Detection of clouds in Antarctica from infrared multispectral data of AVHRR, *J. Meteor. Soc. Japan*, **65**: 949–962.



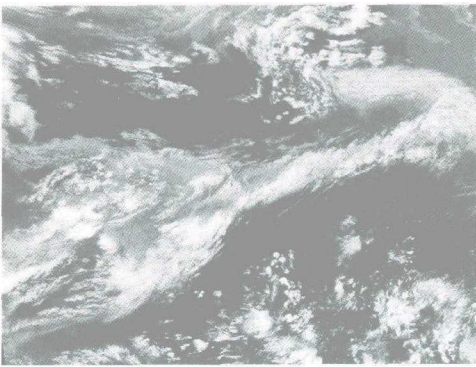
(a)



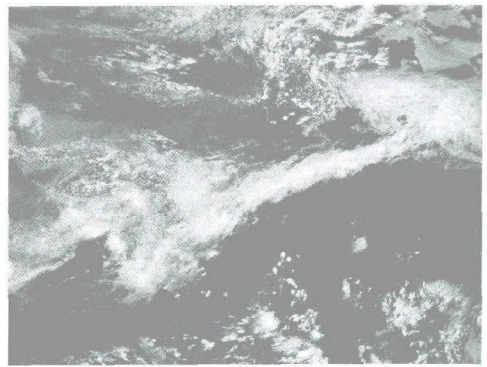
(b)

*Cb Cu con Cu hum Ci middle low land water unknown

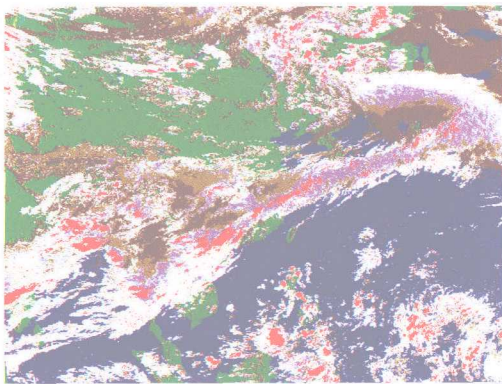
Fig. 1. (a) The NOAA-11 classified color image at 0500 UTC 20 July 1992, the range is 30–35°N, 140–145°E. (b) The Channel-4 cloud image at the same time.



(a)



(b)



(c)

water
 land
 low cloud
 middle cloud
 cirrus
 thin cirrus
 multi-level cloud
 cumulonimbus

Fig. 2. GMS-5 cloud classification images at 0600 UTC 24 June 1999 for (a) IRI, (b) VIS and (c) color image.

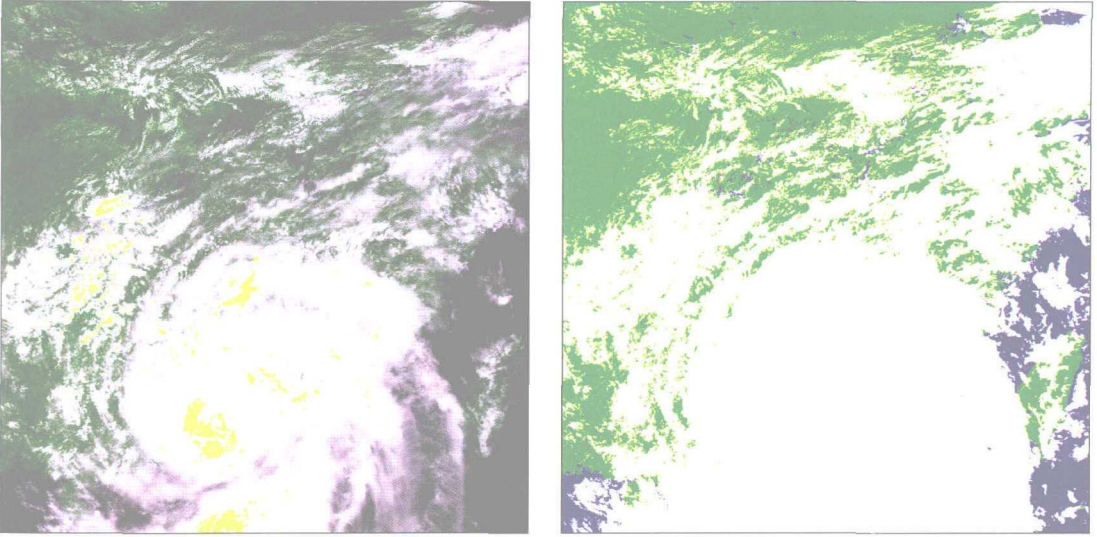


Fig. 3. An example of the cloud mask using MODIS data over China (6 July 2001). The left image is combination by Channels 1, 2 and 4, and the right one is cloud mask image, green regions are land, blue regions are water, white areas are cloudy.

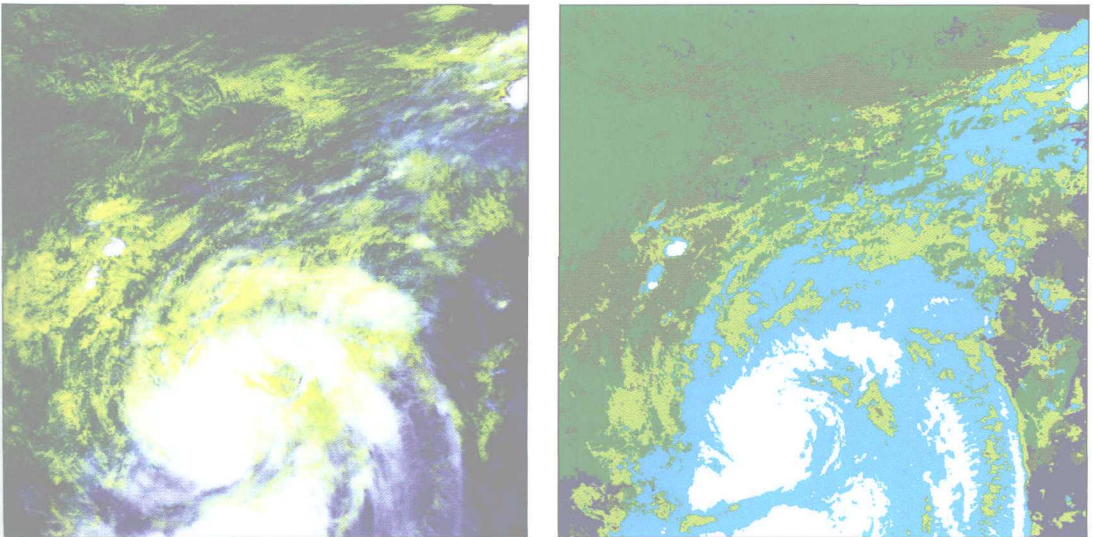


Fig. 4. An example of the cloud classification using MODIS data over China (6 July 2001). The left image is the composed image of bands 1, 2 and 31 and the right one is a cloud classified imagery. In the cloud classified imagery, the green regions are land, blue regions are water, white cumulonimbus, cyan areas are cirrus, and dark yellow areas are low-level cloud.